16

Photocatalytic methyl orange degradation on the surface of nanoporous layers of copper, silver and their iodides

© P.A. Bezrukov[1], A.V. Nashchekin[2], A.I. Sidorov[1,3], H.V. Nikonorov[1]

[1] ITMO University,
197101 St. Petersburg, Russia
[2] Ioffe Institute,
194021 St. Petersburg, Russia
[3] St. Petersburg State Electrotechnical University „LETI",
St. Petersburg, Russia

e-mail: pawqa1@yandex.ru

Received November 30, 2022
Revised December 29, 2022
Accepted January 28, 2023

The efficiency of photocatalytic decomposition of methyl orange solutions on the surface of nanoporous layers of copper, silver and their iodides has been studied. It is shows that nanoporous layers on metal substrates have two absorption bands: they absorb radiation in the UV and Vis spectral range. The process of decomposition of methyl orange molecules on the surface of metal-semiconductor nanostructures Ag−AgI and Cu−CuI occurs under the action of UV and Vis irradiation. While transparency of the methyl orange solution increases.

Keywords: nanoporous layer, nanostructures metal-semiconductor, methyl orange, decomposition, photocatalysis.

DOI: 10.61011/EOS.2023.02.55789.16-23

Introduction

Photocatalytic water splitting is a promising method of solar energy utilization. During water decomposition induced by solar light, gaseous hydrogen and oxygen are formed. Oxygen is extensively used in chemical, glass, food industry, while hydrogen is used as hydrogen fuel to reduce „transport carbon footprint" [1–3]. Hydrogen fuel cells have higher efficiency compared with alternative energy source cells: solar and wind [4–6]. For hydrogen production, an important environment-friendly benefit of the photocatalytic water splitting is that generation of associated gases, except oxygen, is avoided. Therefore, the obtained hydrogen is considered „green" [7]. Pharmaceutical, textile and paper industries discharge colored waste water leading to considerable environment pollution. Contaminants harmful for human body and environment are damaged by high-activity hydroxyl groups which may be generated at one of the photocatalytic water decomposition stages. [8].

Photocathode absorbing the photon energy and providing electron transport into electrolyte is the key component of solar-induced water decomposition systems. photocathodes are traditionally made from silver, gold and copper — high-conductivity materials. Semiconductor photocatalysts are widely used for hydrogen and oxygen generation: ZrO_2, ZnO, WO_3, TiO_2, AgHal, $CuHal_2$ [9–12]. Their performance depends not only on the photocathode material, but also on photocathode surface morphology. Nanoporous materials have high work surface/volume ratio and, therefore, their utilization as photocathodes increases water splitting efficiency and ensures their high potential for photocatalytic processes. On the other hand, work mechanism of nanoporous conducting materials is understudied, only a low number of nanoporous film efficiency investigations is available in literature [13].

The purpose of this study was to investigate the ability of photocatalysts - thin nanoporous copper, silver and their iodide layers — to discolor aqueous solutions of methyl orange (MO) dyes and methylene blue when exposed to UV and visible spectrum radiation.

Procedure and materials

Synthesis of nanoporous copper, silver and iodide films

Thin nanoporous silver and copper films were synthesized by substitution reaction from silver nitrate aqueous (37.5 g/l) and cuprous sulphate (50 g/l) on copper and iron substrates, respectively, degreased in alcohol and dried [14]:

$$Fe + CuSO_4 \rightarrow Cu\downarrow + FeSO_4,$$

$$Cu + 2AgNO_3 \rightarrow 2Ag\downarrow + Cu(NO_3)_2.$$

This method of thin nanoporous copper and silver film production features high synthesis rate, availability of necessary materials and synthesized photocatalyst scaling. Iodization of nanoporous copper and silver layers was performed during 10 min in iodine vapor at room temperature.

Dye solution preparation

10 mg/l of MO was dissolved in distilled water.

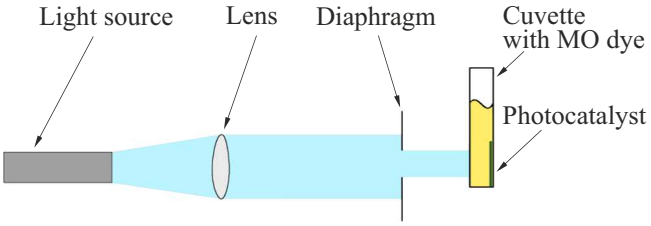

Figure 1. Irradiation system components diagram.

Nanoporous film study

Analysis of specimen surface morphology was carried out by scanning-electron microscopy method using JSM 7001F microscope (Jeol, Japan). Diffusion reflection spectra of thin silver and copper films were measured using Lambda 900 spectrophotometer (PerkinElmer, USA). Optical density spectra of dye solutions were measured using Lambda 650 spectrophotometer (PerkinElmer, USA). photocatalytic activity of specimens was estimated by degradation of dyes exposed to Exfo Novacure 2100 mercury fiber source (Artisan, USA) in spectral range 320–500 nm. Density of source radiation power that has reached the specimens was equal to 30 mW/cm^2.

Dye solution discoloration efficiency study

Synthesized nanoporous copper and silver film specimens were held in darkness during 30 min in dye solution in order to achieve adsorption-desorption balance on the specimen surface.

Dye solution was exposed to visible and UV radiation in the presence/absence of photocatalysts with periodic measurements (every 10 min) of dye solution temperature and volume, optical characteristics in spectral range 300–600 nm.

Figure 1 shows irradiation system components diagram. Collecting lens is placed at a focal distance from the light source for beam collimation. The diaphragm diameter is 2 mm. Power density falling on the specimen may be controlled by the distance between the cuvette and light source. With reduction of this distance, the solution is heated. Therefore, water evaporates and increases dye concentration and introduces errors into the results [12]. Mutual arrangement of components (Figure 1) prevented water evaporation. The specimen was irradiated at room temperature 21°C and power density 30 mW/cm^2. Solution temperature variation did not exceed 2°C. Focal distance of the lens is 80 mm. The distance between the diaphragm and specimen in the cuvette is 28 mm.

Dye degradation C/C_0 was calculated as the ratio of optical density of dye with concentration C at a certain time to the dye density with initial concentration C_0 at 465 nm.

Photocatalytic efficiency D is calculated using the equation

$$D = \frac{C_0 - C}{C_0} 100\%.$$

Zero-, first- and second-order reaction kinetics was used to study MO degradation on the photocatalyst surfaces. Individual equations are as follows [15]:

zero-order reaction kinetics k_0:

$$\frac{dC}{dt} = -k_0, \tag{1}$$

first-order reaction kinetics k_1:

$$\frac{dC}{dt} = -k_1 C, \tag{2}$$

second-order reaction kinetics k_2:

$$\frac{dC}{dt} = -k_2 C^2, \tag{3}$$

where C is the MO concentration at time t; k_0, k_1, k_2 are apparent zero-, first- and second-order reaction kinetic constants, respectively.

After integration and regression analysis based on zero-, first- and second-order reaction kinetics of MO decomposition on the photocatalyst surfaces, regression coefficients R^2 were defined. R^2 — is the approximation integrity of trend line of MO concentration variation vs. irradiation time [15].

Findings and discussion

Study of thin nanoporous silver and copper film specimens

Synthesized nanoporous copper layer (Figure 2, *a*) consists of microdendrites with sizes up to 5 μm, on which dendrite-like buildups with sizes up to 400 nm formed. Nanoporous silver layer (Figure 2, *b*) consists of hexagonal plates with sizes up to 2 μm. Micro- and nanodendrites with sizes 3 μm and 100 nm, respectively, are also present.

In iodine vapor at room temperature during 10 min, nanoporous metal layer partially transforms into metal iodide. Specimen color changed from grayish-white (silver nanoporous layer) to yellowish-white and from dark-brown (copper nanoporous layer) to yellowish-brown. Partial iodination results in synthesis of nanostructured metal-semiconductor type composite: Ag–AgI and Cu–CuI. Electron-hole pairs formed on the semiconductor surface are involved in the dye decomposition reaction.

Diffusion reflection (Figure 3) of silver nanoporous layer is lower than nanoporous copper layer reflection. A larger number of photons is absorbed on the nanoporous silver layer than on the nanoporous copper layer.

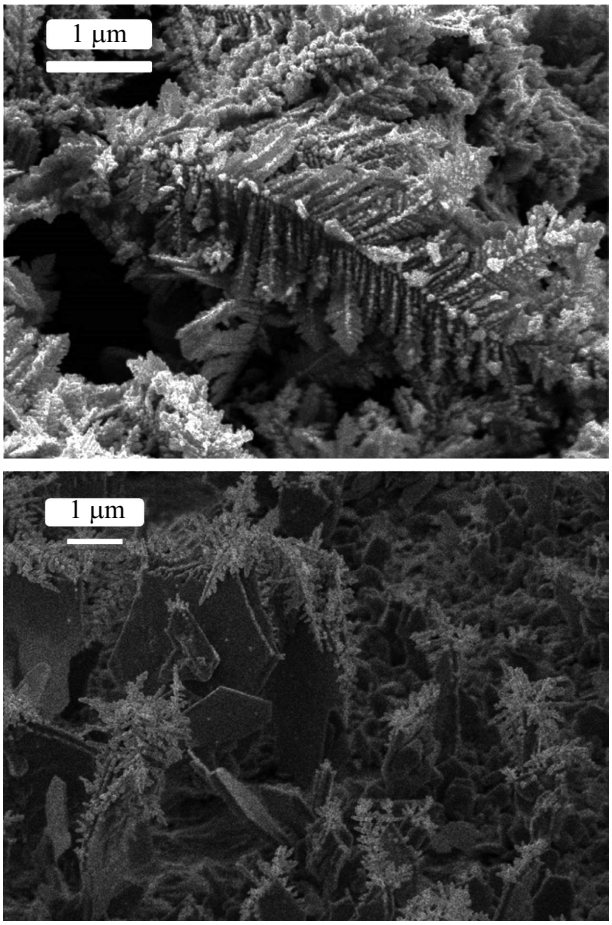

Figure 2. SEM images of nanoporous layers: (*a*) copper, reaction time is 4 s, (*b*) silver, reaction time is 4 s.

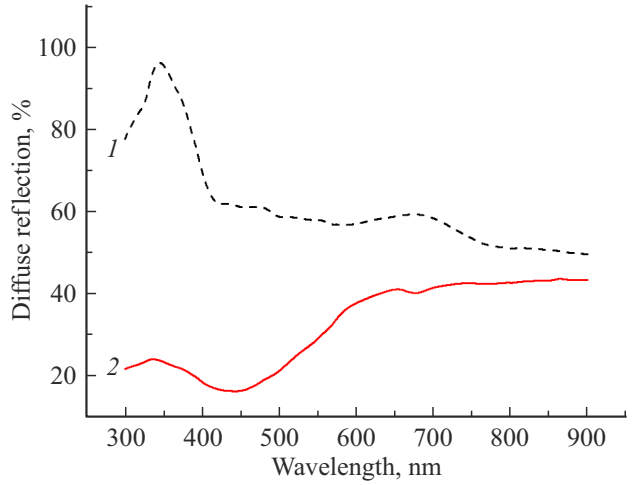

Figure 3. Diffusion reflection of nanoporous copper (*1*) and silver (*2*) layers.

Dye solution discoloration efficiency study

Figure 4 shows optical density spectra of MO solution irradiated in the presence of Cu−CuI. Presence of MO molecules in the solution is characterized by azo-group (-N=N-) in the molecule structure with absorption peak in the wavelength range 460−465 nm. Absorption peak at 464 nm, when exposed to irradiation, gradually decreases with the increase in irradiation time, which is indicative of MO molecule decomposition and formation of simple compounds with amine groups.

No pronounce photodegradation of MO without photocatalyst and on the surface of nanoporous silver layers occurs under exposure to irradiation with power density 30 mW/cm^2 (Figure 5). Nanoporous metal-semiconductor layers demonstrate higher photocatalytic activity than nanoporous silver and copper layers and discolor $20 \pm 0.6\%$ (AgI) and $35 \pm 0.9\%$ (CuI) of MO during 60 min, respectively. confidence error was equal to 2.8% (Table 1). Electron-hole pairs appear on the photocatalyst surface. Formed electrons are removed from Ag−AgI and Cu−CuI interface and are captured by O_2 in the solution with

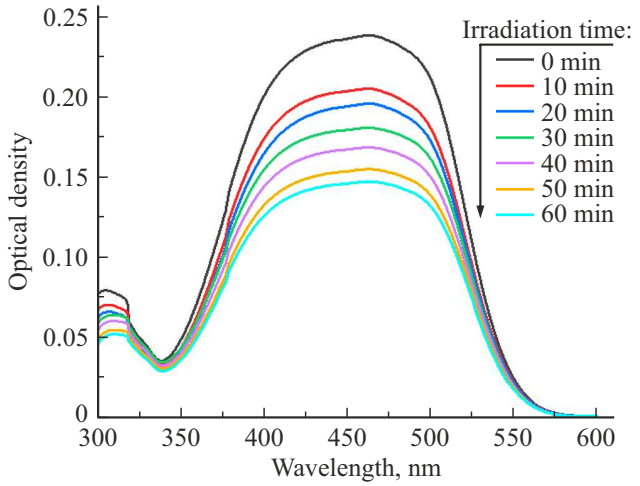

Figure 4. MO solution absorption spectra after UV and visible spectrum irradiation in the presence of Cu−CuI composite.

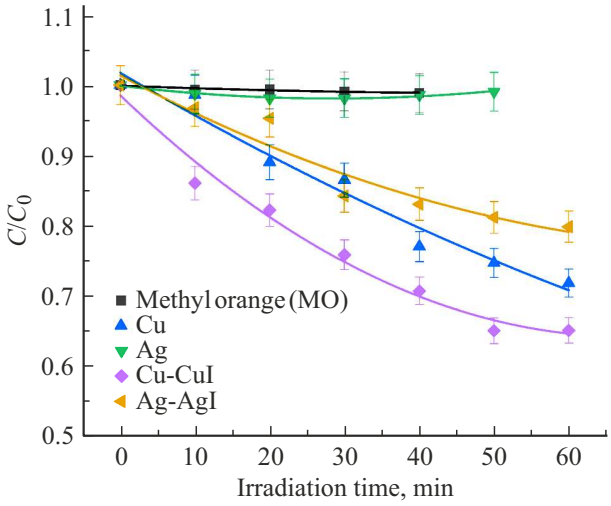

Figure 5. MO concentration in aqueous solution vs. irradiation time.

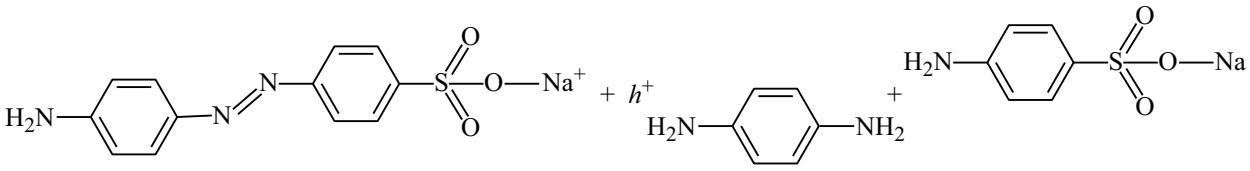

Diagram. MO molecule interaction with hole with formation of simple amine containing compounds.

Table 1. photocatalytic efficiency D of MO decomposition on the nanoporous catalyst film surfaces during 60 min

Photocatalyst	D, %
Ag	1
Cu	28
Ag−AgI	20
Cu−CuI	35

Table 2. Regressive coefficients of MO photocatalytic decomposition reaction kinetics vs. irradiation time

Kinetics kinetics reaction order	Integrated equation	R^2 (Cu−CuI)	R^2(Ag−AgI)
Zero	$C(t)$, mg·l^{-1}·min^{-1}	0.9592	0.9113
First	$\mathrm{Ln}(C/C_0)(t)$	0.9812	0.9159
Second	$1/C(t)$, l·mg^{-1}	0.9914	0.9202

generation of superoxide anion radicals O_2^-. And oles on AgI and CuI surfaces take part in MO molecule decomposition reaction into simple compounds with amine groups (diagram).

Appearing anion radicals $\bullet O_2$ also take part in the dye molecule destruction and MO solution discoloration reaction [16–18]. Cu−CuI surface contains partially iodinated micro- and nanodendrites (Figure 2, *a*). Nanoporous Ag−AgI layer surface contains nanodendrites and silver polygons (Figure 2, *b*). Sharp edges of polygons are iodinated at first, therefore the main array consists of silver plates. Nanoporous Cu−CuI layer surface contains a large number of reaction centers due to more developed metal-semiconductor surface, therefore the photocatalytic efficiency of dye decomposition in the presence of copper iodide is higher compared with silver iodide.

Regressive coefficient R^2 (Table 2) of the second-order kinetics reaction is equal to 0.9914 (for Cu−CuI) and to 0.9202 (for Ag−AgI), which exceeds corresponding regressive coefficients R^2 of the zero- and first-order kinetics reactions. MO decomposition reaction on the photocatalyst surface flows according to the second-order equation which describes adsorption process flow in gas/solid body and solution/solid body systems [19].

Conclusions

It is shown that nanostructured silver films are not effective for dye molecule decomposition and, thus, for decomposition of waste water contaminations. Nanoporous copper and Cu−CuI and Ag−AgI films are no longer suitable for decontamination of waste water even at low power of light source. Nanostructured Cu−CuI and Ag−AgI decompose MO and discolor solutions by 35±0.9% and 20±0.6% during 60 min, respectively.

It has been found that transformation of nanoporous metal layer to metal-semiconductor type composite (Ag−AgI and Cu−CuI) increases photocatalytic activity of MO decomposition. For Ag−AgI, photocatalytic efficiency is increased by a factor of more than 20. For Cu−CuI, the increase was by a factor of 1.25.

The findings have shown that MO degradation kinetics on Cu−CuI and Ag−AgI surface corresponds to the second-order kinetics.

Acknowledgments

The electron microscopic study was performed using the equipment provided by the Federal SUC „Materials Science and Diagnostics in Advanced Technologies“, supported by the Ministry of Education and Science of Russia.

Funding

This study was financially supported by the Russian Science Foundation (project № 20-19-00559).

Conflict of interest

The authors declare that they have no conflict of interest.

References

[1] S. Markgraf, M. Horenz, T. Schmiel, W. Jehle, J. Lucas, N. Henn. J. Power Sources, **201**, 236 (2012). DOI: 10.1016/j.jpowsour.2011.10.118

[2] K. Maeda. J. Photochem. Photobiol. C., **12**, 237 (2011). DOI: 10.1016/j.jphotochemrev.2011.07.001

[3] Y. Wang, D. He, D. Wang. J. Photochem. Photobiol. C., **40**, 117 (2019). DOI: 10.1016/j.jphotochemrev.2011.07.001

[4] M. Mitra. Electr. Eng. Op. Acs. Open J., **1** (1), 1 (2019). DOI: 10.5281/zenodo.2616442

[5] P.P. Kundu, K. Dutta. *Compendium of Hydrogen Energy* (Woodhead Publishing, Oxford, 2016), 4. DOI: 10.1016/B978-1-78242-364-5.00006-3

[6] Z. Zhang, F. Li, H. Feng, C. Ma, X. Hou. In: E3S Web Conf. (ICAEER 2019), v. 118, p. 01058. DOI: 10.1051/e3sconf/201911801058
[7] M.Kh Sosna, M.V. Kryuchkov, M.V. Maslennikova, M.V. Pustovalov. NefteGasoKhimiya, **3** (4), 21 (2020) (in Russian). DOI: 10.24412/2310-8266-2020-3-4-21-23
[8] Y. Ahmed, Z. Yaakob, P. Akhtar. Catal. Sci. Technol., **6** (4), 1222 (2016). DOI: 10.1039/c5cy01494h
[9] X. Fu, H. Chang, Z. Shang, P. Liu, J. Liu, H. Luo. Chem. Eng. J., 381, 122001 (2020). DOI: 10.1016/j.cej.2019.122001
[10] L. Wang, W. Si, X. Hou, M. Wang, X. Liu, Y. Ye, F. Hou, J. Liang. Sust. Mater. Technol., **25**, e00209 (2020). DOI: 10.1016/j.susmat.2020.e00209
[11] Z. Liu, W. Hou, P. Pavaskar, M. Aykol, S.B. Cronin. Nano. Lett., **11** (3), 1111 (2011). DOI: 10.1021/nl104005n
[12] Q. Hu, L. Baoshun, Z. Zhang, M. Song, X. Zhao. J. Wuhan Univ. Technol.-Mat. Sci. Edit., **25** (2), 210 (2010). DOI: 10.1007/s11595-010-2210-5
[13] M. Graf, D. Jalas, J. Weissmuller, A.Y. Petrov, M. Eich. ACS Catal., **9** (4), 3366 (2019). DOI: 10.1021/acscatal.9b00384
[14] P.A. Bezrukov, A.V. Nashchekin, N.V. Nikonorov, A.I. Sidorov. Nauch.-Tekhn. Vestnik Inform. Tekhn., Mekh. i Opt., **21** (4), 457 (2021) (in Russian). DOI: 10.17586/2226-1494-2021-21-4-457-462
[15] N. Youssef, S. Shaban, F. Ibrahim, A. Mahmoud. Egypt. J. Petroleum, **25** (3), 317 (2016). DOI: 10.1016/j.ejpe.2015.07.017
[16] J. Xiong, Z. Li, S. Zhang, L. Wang, S. Dou. ACS Appl. Mater Interfaces, **6** (18), 15716 (2014). DOI: 10.1021/am502516s
[17] P. Wang, B. Huang, Q. Zhang, X. Zhang, X. Qin, Y. Dai, J. Zhan, J. Yu, H. Liu, Z. Lou. Chem. Eur. J., **16**, 10042 (2010). DOI: 10.1002/chem.200903361
[18] J. Jiang, L. Zhang. Chem. Eur. J., **17**, 3710 (2011). DOI: 10.1002/chem.201002951
[19] Y-S. Ho, J. Hazard. Mat., **136** (3), 681 (2006). DOI: 10.1016/j.jhazmat.2005.12.043

Translated by E.Ilyinskaya